

# On the Operation Mechanism and Device Modeling of AlGa<sub>N</sub>/Ga<sub>N</sub> High Electron Mobility Transistors (HEMTs)

Li Yuan, Weizhu Wang, Kean Boon Lee, Haifeng Sun, Susai Lawrence Selvaraj, Shane Todd, Guo-Qiang Lo

**Abstract**—In this work, the physical based device model of AlGa<sub>N</sub>/Ga<sub>N</sub> high electron mobility transistors (HEMTs) has been established and the corresponding device operation behavior has been investigated also by using Sentaurus TCAD from Synopsys. Advanced AlGa<sub>N</sub>/Ga<sub>N</sub> hetero-structures with Ga<sub>N</sub> cap layer and AlN spacer have been considered and the Ga<sub>N</sub> cap layer and AlN spacer are found taking important roles on the gate leakage blocking and off-state breakdown voltage enhancement.

**Keywords**—AlGa<sub>N</sub>/Ga<sub>N</sub>, HEMT, Physical mechanism, TCAD simulation

## I. INTRODUCTION

THREE-nitride wide-bandgap materials, e.g. Ga<sub>N</sub>, AlN attract a lot of attentions owing to their material advantages. Especially, AlGa<sub>N</sub>/Ga<sub>N</sub> hetero-junction based high electron mobility transistors (HEMTs) can provide both low on-resistance and high off-state breakdown voltage simultaneously, possessing unique device characteristics for power electronics applications.

Tremendous progress has been made in AlGa<sub>N</sub>/Ga<sub>N</sub> HEMT technology [1-3], however, a complete physical based device model of AlGa<sub>N</sub>/Ga<sub>N</sub> HEMTs is still highly desired, which can be used to reveal the transistors' unique physical mechanisms and predict the device operation behavior.

In this work, a physical based device simulation of AlGa<sub>N</sub>/Ga<sub>N</sub> HEMTs has been carried out by using Sentaurus TCAD from Synopsys. Pivotal physical mechanisms, such as gate Schottky tunneling, surface cap layer leakage, avalanche breakdown and Ga<sub>N</sub> buffer leakage can be revealed. According to device simulation, the switching on/off behavior, on-state output characteristics and off-state breakdown of AlGa<sub>N</sub>/Ga<sub>N</sub> HEMTs can be modeled. Ga<sub>N</sub> cap layer and AlN spacer are suggested to be implemented into the standard AlGa<sub>N</sub>/Ga<sub>N</sub> hetero-structure to suppress the gate leakage and to enhance both the off-state breakdown voltage and on-state current driving capability.

## II. DEVICE STRUCTURE AND MODELING SETUP

For the device simulation, the standard AlGa<sub>N</sub>/Ga<sub>N</sub> HEMTs on high resistivity Si wafer have been modeled as shown in Fig. 1. From top to bottom, the hetero-structure consists of an Al<sub>0.24</sub>Ga<sub>0.76</sub>N barrier layer (20 nm), a Ga<sub>N</sub> buffer layer (3 μm), an AlGa<sub>N</sub>/AlN transition/nucleation layer (1 μm) and the Si substrate (1 μm).

Authors are with the Institute of Microelectronics, A\*STAR (Agency for Science, Technology and Research), 11 Science Park Road, Singapore Science Park II, Singapore 117685 (phone: +65-6770 5603; fax: +65-6773 1914; e-mail: yuanl@ime.a-star.edu.sg).

This work is supported by TSRP SERC "Ga<sub>N</sub>-on-Si Power Electronics Program" with the Project code of 102 169 0126.

The unintentional background n-type doping in AlGa<sub>N</sub> and Ga<sub>N</sub> layer is set to be  $10^{16} \text{ cm}^{-3}$  [4], and the Fe compensation doping ( $2 \times 10^{17} \text{ cm}^{-3}$ ) in Ga<sub>N</sub> buffer [5] is also considered. High density donor-like traps are added in the AlGa<sub>N</sub>/AlN transition/nucleation layer to model the lattice dislocations. The Si layer here is un-doped to model the high-resistivity substrate.

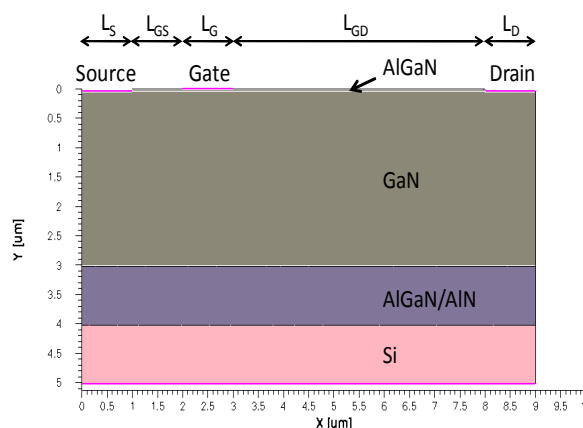


Fig. 1 The cross-section view of AlGa<sub>N</sub>/Ga<sub>N</sub> HEMT device model structure

Three different barrier structures on top of the Ga<sub>N</sub> buffer have been modeled in our work, (a) the standard AlGa<sub>N</sub> barrier, (b) the AlGa<sub>N</sub> barrier with 2 nm Ga<sub>N</sub> cap layer and (c) the AlGa<sub>N</sub> barrier with 2 nm Ga<sub>N</sub> cap layer and 1 nm AlN spacer.

Same device geometries with Ni gate length of 1 μm, source/drain ohmic contact length of 1 μm,  $L_{GS}$  of 1 μm and  $L_{GD}$  of 5 μm are used in our simulation.

In our device simulation, the Sentaurus TCAD v2010.03 software is used. The simulated conduction band diagram of AlGa<sub>N</sub>/Ga<sub>N</sub> hetero-junction is shown in Fig. 2. With the lattice stress relax of 10%, the spontaneous and piezoelectric polarization of the AlGa<sub>N</sub>/Ga<sub>N</sub> hetero-junction are  $0.78 \times 10^{13} \text{ cm}^{-2}$  and  $0.51 \times 10^{13} \text{ cm}^{-2}$ , respectively.

On the surface of AlGa<sub>N</sub> barrier, there are donor-like surface states of  $\sim 10^{13} \text{ cm}^{-2}$  arising from the Ga adatom dangling bonds [6]. In our simulation, the AlGa<sub>N</sub> surface trap state is set to be located at 3.2 eV above the valance band. The distribution of electron carriers within the AlGa<sub>N</sub>/Ga<sub>N</sub> hetero-junction is shown in Fig. 3.

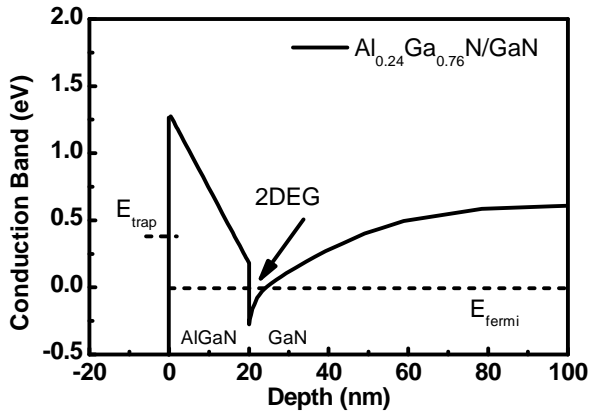


Fig. 2 The conduction band diagram of AlGaIn/GaN hetero-junction

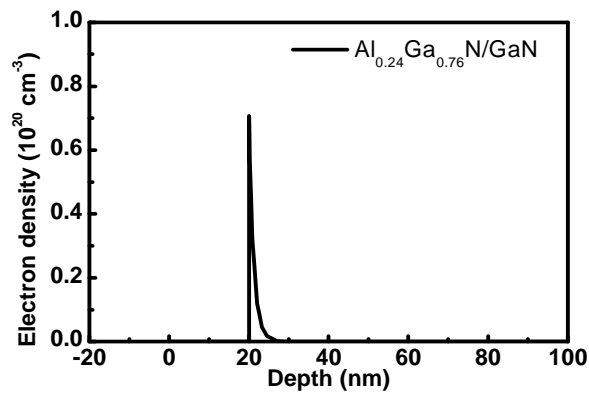


Fig. 3 The electron carrier distribution profile within the AlGaIn/GaN hetero-junction

The conduction band structures of AlGaIn/GaN hetero-junction under Ni gate Schottky contact are calculated and shown in Fig. 4. The influence of GaN cap layer and AlN spacer are also taken into account. As we can see, the conduction band of GaN cap layer is lower than AlGaIn barrier, due to the material properties. In addition, with the polarization effect between AlGaIn and GaN, both two dimensional electron gas (2DEG) and two dimensional hole gas (2DHG) will be formed. The AlN spacer can provide an additional energy barrier between AlGaIn/GaN and enhance both the electron carrier mobility and concentration [8].

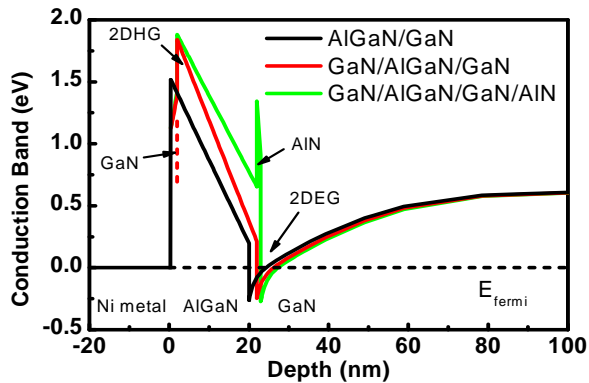


Fig. 4 The conduction band diagram of AlGaIn/GaN hetero-junction with GaN cap layer and AlN spacer under the Ni gate metal contact

### III. RESULTS AND DISCUSSIONS

The transfer  $I_{DS}$ - $V_{GS}$  characteristics of standard AlGaIn/GaN HEMT, HEMT with GaN cap layer and HEMT with GaN cap and AlN spacer are shown in Figs. 5 and 6. As we can see, the standard HEMT suffers both higher gate and drain off-state leakage current compared to the HEMT with GaN cap layer. The current density distribution profiles of standard AlGaIn/GaN HEMT at  $V_{GS} = -6$  V and  $V_{DS} = 10$  V are plotted in Figs. 7 and 8, indicating the domination of the leakage behavior of standard AlGaIn/GaN HEMT by the gate leakage current, especially at the drain side gate edge.

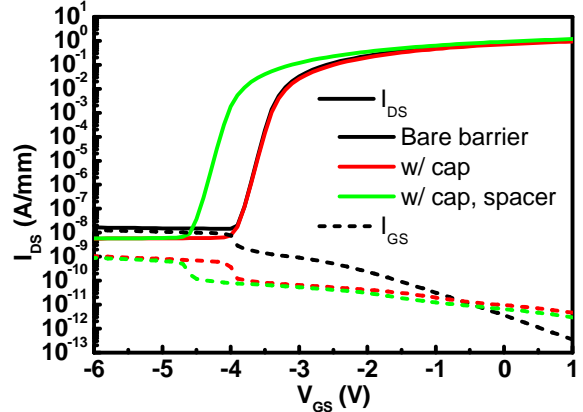


Fig. 5 The simulated  $I_{DS}$ - $V_{GS}$  transfer characteristics of standard AlGaIn/GaN HEMT, HEMT with GaN cap layer and HEMT with GaN cap and AlN spacer in log scale

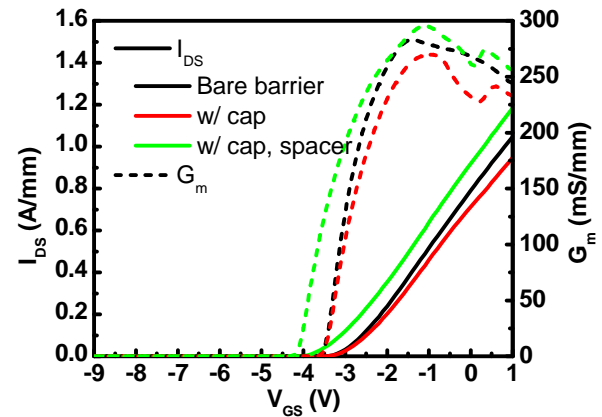


Fig. 6 The simulated  $I_{DS}$ - $V_{GS}$  and  $G_m$ - $V_{GS}$  transfer characteristics of standard AlGaIn/GaN HEMT, HEMT with GaN cap layer and HEMT with GaN cap and AlN spacer in linear scale

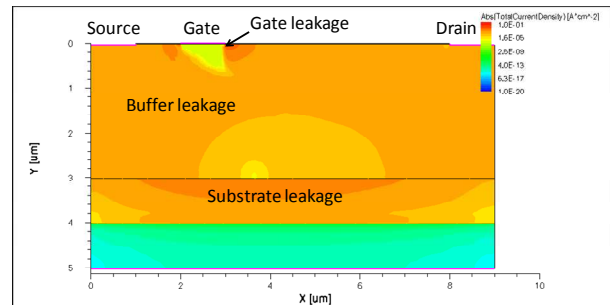


Fig. 7 The current density distribution profile of AlGaIn/GaN HEMT at  $V_{GS} = -6$  V and  $V_{DS} = 10$  V

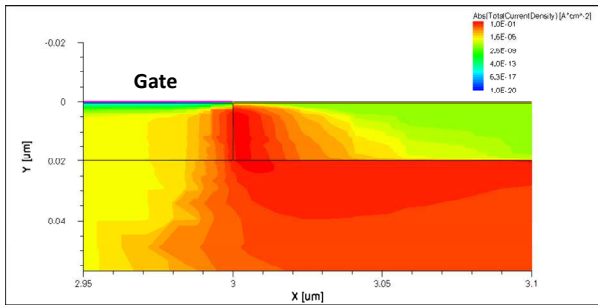


Fig. 8 The zoom-in current density distribution profile of AlGaIn/GaN HEMT at  $V_{GS} = -6$  V and  $V_{DS} = 10$  V

In the off-state, the gate Schottky contact is reverse biased, thus the gate current will be composed of the gate tunneling and thermionic emission current. The distribution of gate tunneling rate is plotted in Fig. 9, which shows a strong electron tunneling close to the drain side gate edge and is consistent with the gate leakage current distribution shown in Fig. 8. Fig. 10 shows the conduction band energy level distribution in standard AlGaIn/GaN HEMT at  $V_{GS} = -6$  V and  $V_{GS} = 10$  V. As we can see, the positively biased drain electrode can pull down the conduction band level between gate and drain, thus at the drain side gate edge, the voltage drop between the gate contact and the 2DEG channel will be higher than the one under the gate electrode and far from the drain, therefore the strongest electron carrier tunneling will occur at the drain side gate edge.

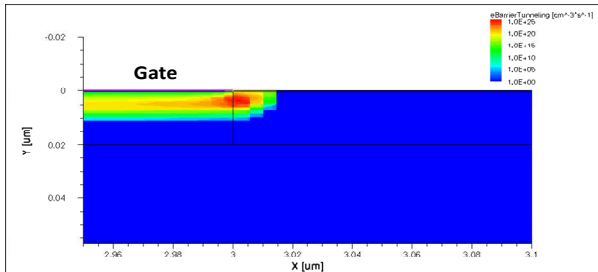


Fig. 9 The zoom-in gate electron tunneling distribution profile of AlGaIn/GaN HEMT at  $V_{GS} = -6$  V and  $V_{DS} = 10$  V

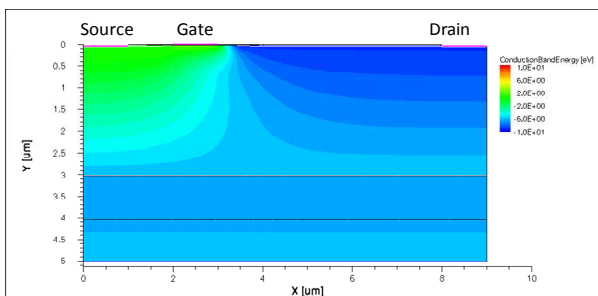


Fig. 10 The conduction band distribution profile of AlGaIn/GaN HEMT at  $V_{GS} = -6$  V and  $V_{DS} = 10$  V

When AlGaIn/GaN HEMT is capped by the GaN layer, the gate tunneling current can be suppressed, due to the virtual gate screen effect [9, 10] induced by the surface leakage current along the GaN cap layer, as shown in Fig. 11.

The AlGaIn/GaN HEMT with GaN spacer and AlN spacer delivers higher current driving capability and more negative threshold voltage compared to the standard AlGaIn/GaN HEMT, owing to the higher 2DEG channel mobility and carrier concentration. The output characteristics of standard AlGaIn/GaN HEMT, HEMT with GaN cap layer and HEMT with GaN cap and AlN spacer are plotted in Fig. 12.

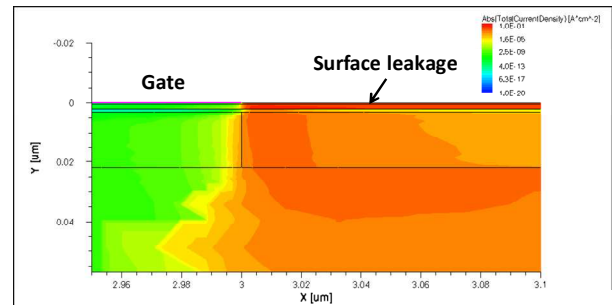


Fig. 11 The zoom-in current density distribution profile of AlGaIn/GaN HEMT with GaN cap layer at  $V_{GS} = -6$  V and  $V_{DS} = 10$  V

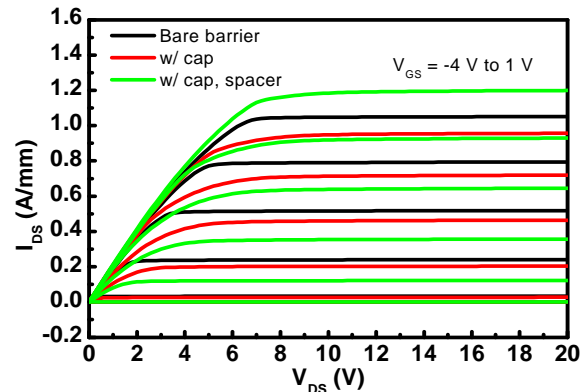


Fig. 12 The simulated  $I_{DS}$ - $V_{DS}$  output characteristics of standard AlGaIn/GaN HEMT, HEMT with GaN cap layer and HEMT with GaN cap and AlN spacer.  $V_{GS}$  sweeps from -4 V to 1 V at a step of 1 V

The off-state  $I_{DS}$ - $V_{DS}$  characteristics of standard AlGaIn/GaN HEMT, HEMT with GaN cap layer and HEMT with GaN cap and AlN spacer are illustrated in Fig. 13. As we can see, the breakdown voltages of three kinds of devices are extracted as 268 V, 705 V and 630 V, respectively. As discussed above, with the assistance of the GaN cap layer, the impact of the drain voltage on the potential distribution between gate and drain can be partially screened by the virtual gate effect. As a result, not only the gate leakage will be suppressed but also the electrical field distribution can be uniformed (Fig. 14), compared to the standard AlGaIn/GaN HEMT. Therefore, HEMTs with GaN cap layer can deliver higher breakdown voltage. In addition, the breakdown voltage of AlGaIn/GaN HEMT with AlN spacer will be slightly lower than GaN capped HEMT without AlN spacer, due to the higher 2DEG carrier concentration and corresponding shorter depletion length. The off-state conduction band distribution profile of standard AlGaIn/GaN HEMT and HEMT with GaN cap and AlN spacer are compared in Fig. 15.

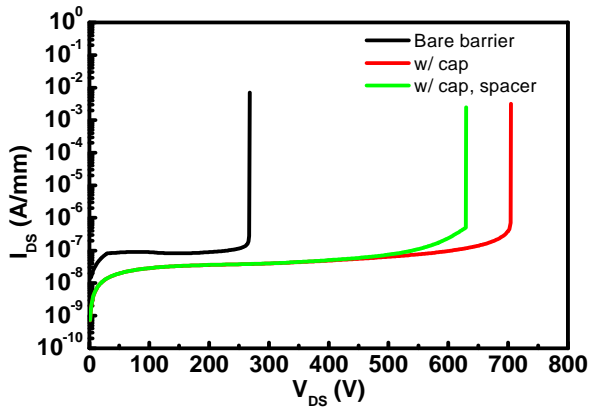


Fig. 13 The simulated  $I_{DS}$ - $V_{DS}$  output characteristics of standard AlGaIn/GaN HEMT, HEMT with GaN cap layer and HEMT with GaN cap and AlN spacer at  $V_{GS} = -5.5$  V

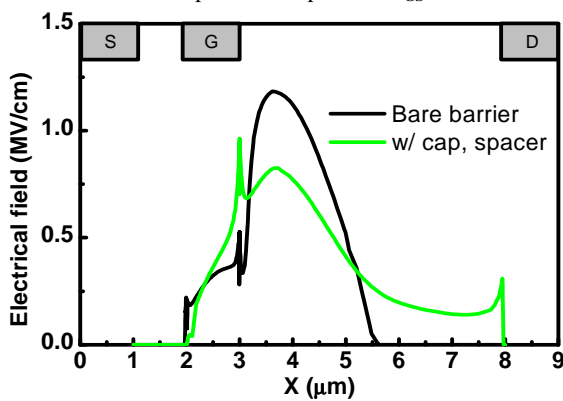


Fig. 14 The electrical field distribution profile in the 2DEG channel of standard AlGaIn/GaN HEMT and HEMT with GaN cap and AlN spacer at  $V_{GS} = -5.5$  V and  $V_{DS} = 200$  V

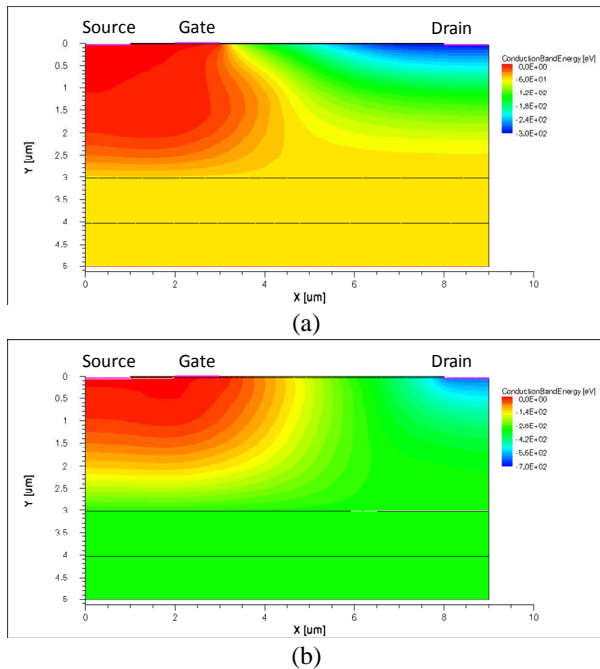


Fig. 15 The conduction band distribution profile of (a) standard AlGaIn/GaN HEMT at  $V_{GS} = -5.5$  V and  $V_{DS} = 268$  V (b) AlGaIn/GaN HEMT with GaN cap and AlN spacer at  $V_{GS} = -5.5$  V and  $V_{DS} = 630$  V

#### IV. CONCLUSION

The device models of AlGaIn/GaN HEMTs have been built and the corresponding device simulations have been carried out by using Sentaurus TCAD tools. It has been found the gate tunneling at the drain side gate edge dominates the off-state leakage current of AlGaIn/GaN HEMTs. With the GaN cap layer, in AlGaIn/GaN HEMTs both the off-state leakage current and peak electrical field strength can be reduced owing to the virtual gate screen effect induced by the surface current in the GaN cap layer, thus higher breakdown voltage can be achieved. Thanks to the higher 2DEG channel carrier mobility and concentration, the AlGaIn/GaN HEMTs with GaN cap and AlN spacer can deliver both better on-state current driving capability and off-state breakdown voltage compared to the standard HEMTs.

#### REFERENCES

- [1] S. Khandelwal, et al., "A Physics-Based Analytical Model for 2DEG Charge Density in AlGaIn/GaN HEMT Devices," *IEEE Trans. Electron Devices*, vol. 58, pp. 3622-3625, Oct. 2011.
- [2] N. Ikeda, et al., "GaN Power Transistors on Si Substrates for Switching Applications," *Proceedings of the IEEE*, vol. 98, pp. 1151-1161, Jul. 2010.
- [3] J. W. Chung, et al., "AlGaIn/GaN HEMT With 300-GHz  $f_{max}$ ," *Electron Device Lett.*, vol. 31, pp. 195-197, Mar. 2010.
- [4] A. Armstrong, et al., "Impact of Growth Pressure on Defects in GaN Grown - by Metalorganic Chemical Vapor Deposition," *Compound Semiconductors: Post-Conference Proceedings*, 2003 International Symposium on, pp. 42-48, 2003.
- [5] Y. C. Choi, et al., "The Effect of an Fe-doped GaN Buffer on OFF-State Breakdown Characteristics in AlGaIn/GaN HEMTs on Si Substrate," *IEEE Trans. Electron Devices*, vol. 53, pp. 2926-2931, Dec. 2006.
- [6] A. Rizzi, et al., "Surface and interface electronic properties of AlGaIn(0001) epitaxial layers," *Appl. Phys. A*, vol.87, pp. 505-509, Mar. 2007.
- [7] B. Jogai, "Influence of surface states on the two-dimensional electron gas in AlGaIn/GaN heterojunction field-effect transistors," *J. Appl. Phys.*, vol. 93, pp. 1631-1634, Feb. 2003.
- [8] X. Wang, et al., "MOCVD-grown high-mobility Al<sub>0.3</sub>Ga<sub>0.7</sub>N/AlN/GaN HEMT structure on sapphire substrate," *Journal of Crystal Growth*, vol. 298, pp. 791-793, 2007.
- [9] R. Vetury, "The Impact of Surface States on the DC and RF Characteristics of AlGaIn/GaN HFETs," *IEEE Trans. Electron Devices*, vol. 48, pp. 560-566, Mar. 2001.
- [10] S. Kasai, et al., "Gate Control, Surface Leakage Currents, and Peripheral Charging in AlGaIn/GaN Heterostructure Field Effect Transistors Having Nanometer-Scale Schottky Gates," *Journal of Electronic Materials*, vol. 35, pp. 568-575, Nov. 2006.